

## **Supplementary material**

# **Characterization of Submicron Particles Influenced by Mixed Biogenic and Anthropogenic Emissions Using High-Resolution Aerosol Mass Spectrometry: Results from CARES**

Ari Setyan<sup>1</sup>, Qi Zhang<sup>1\*</sup>, Maik Merkel<sup>2</sup>, W. Berk Knighton<sup>3</sup>, Yele Sun<sup>4</sup>, Chen Song<sup>5</sup>, John E. Shilling<sup>5</sup>, Timothy B. Onasch<sup>6</sup>, Scott C. Herndon<sup>6</sup>, Douglas R. Worsnop<sup>6</sup>, Jerome D. Fast<sup>5</sup>, Rahul A. Zaveri<sup>5</sup>, Larry K. Berg<sup>5</sup>, Alfred Wiedensohler<sup>2</sup>, Bradley A. Flowers<sup>7</sup>, Manvendra K. Dubey<sup>7</sup>, R. Subramanian<sup>8</sup>

<sup>1</sup> Department of Environmental Toxicology, University of California, Davis, CA 95616, United States

<sup>2</sup> Leibniz Institute for Tropospheric Research, 04318 Leipzig, Germany

<sup>3</sup> Montana State University, Bozeman, MT 59717, United States

<sup>4</sup> State Key Laboratory of Atmospheric Boundary Layer and Atmospheric Chemistry, Institute of Atmospheric Physics, Chinese Academy of Sciences, Beijing, China

<sup>5</sup> Pacific Northwest National Laboratory, Richland, WA 99352, United States

<sup>6</sup> Aerodyne Research Inc., Billerica, MA 01821, United States

<sup>7</sup> Los Alamos National Laboratory, Los Alamos, NM 87545, United States

<sup>8</sup> Droplet Measurement Technologies, Boulder, CO 80301, United States

\* Correspondence to: Qi Zhang (dkwzhang@ucdavis.edu)

**Figure S1.** Time series of (a) temperature, relative humidity and broadband solar radiation (from precision spectral pyranometer [PSP]), (b) wind direction colored by wind speed (height: 3m), (c) concentrations of CO<sub>2</sub>, O<sub>3</sub> and NO<sub>x</sub>, (d) monoterpenes, isoprene and sum of methacrolein (Macr) and methyl vinyl ketone (MVK), (e) formaldehyde, methanol and acetone, (f) acetonitrile, benzene and toluene. Shaded regions indicate 23 periods of urban plumes transported from T0 to T1 (orange) and 3 periods subjected to influences from northwesterly wind (green). The remaining periods correspond mainly to downslope flows from the Sierra Nevada to the foothills.

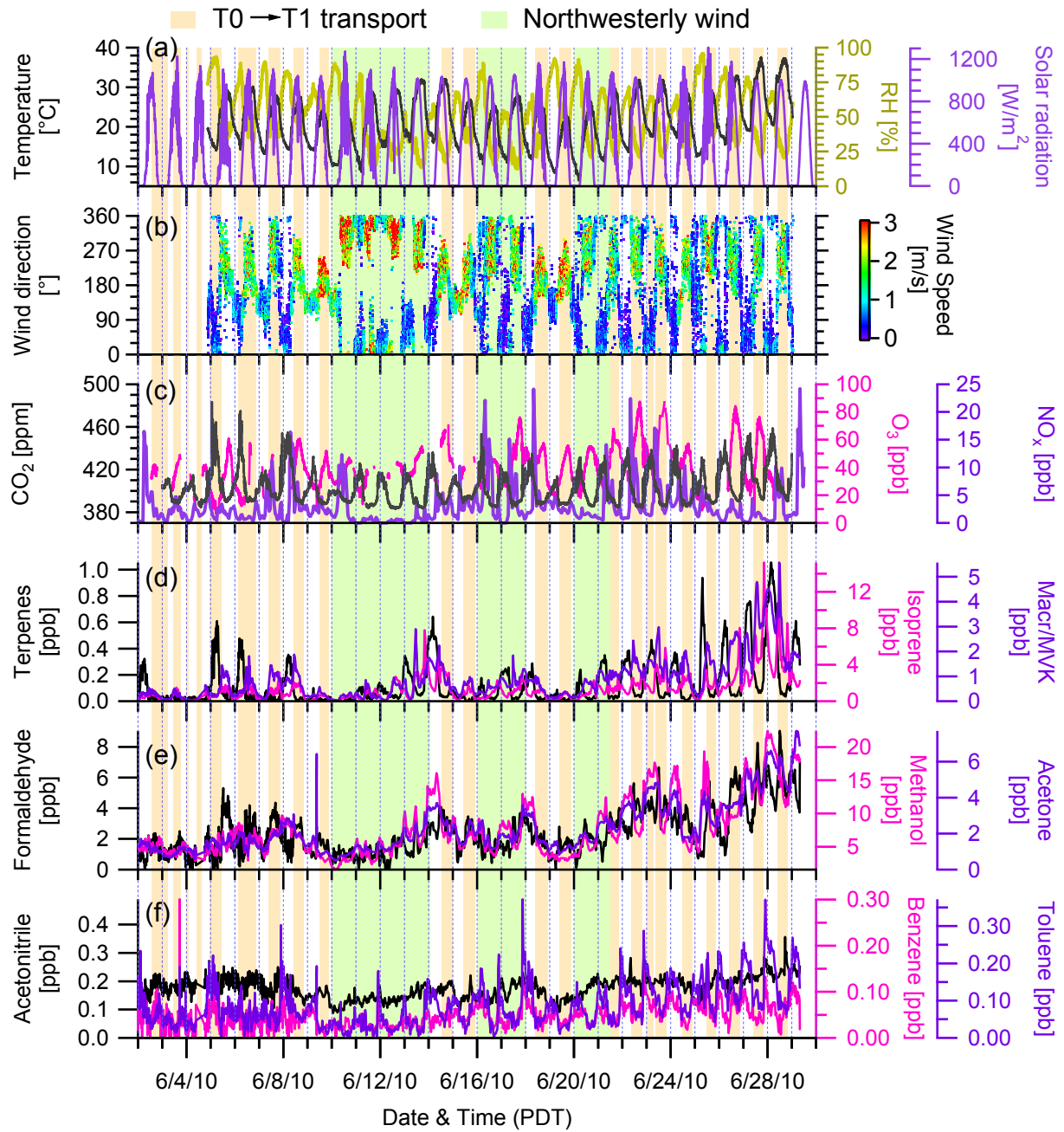


**Figure S2.** Time series of  $\text{NH}_4^+$  using Squirrel and Pika, both in V-mode.

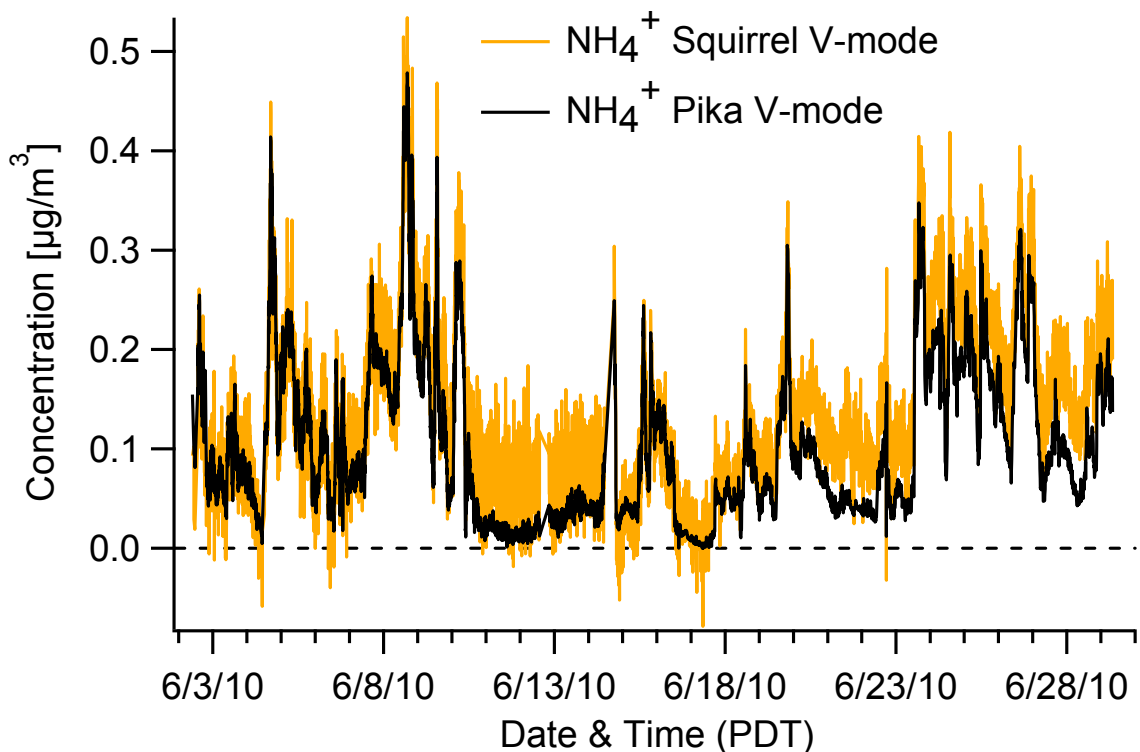


**Figure S3.** Scatterplot of  $\text{CH}_2\text{SO}_2^+$  vs.  $\text{CH}_3\text{SO}_2^+$  (the two main MSA fragments), colored by time. The data fitting was performed using the orthogonal distance regression (ODR).

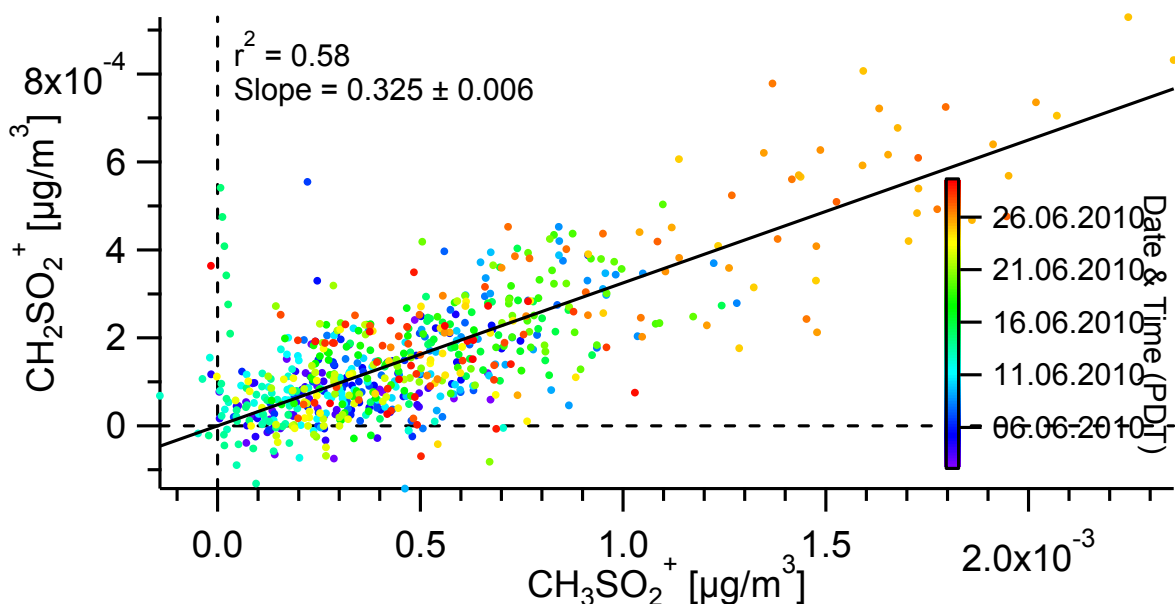


**Figure S4.** Map of the Bay Area and the Sacramento Valley (a). Time series of relative humidity and precipitation recorded at Oakland North (data from the California Air Resources Board) and the T1 site (b). Diurnal pattern of relative humidity at Oakland and the T1 site (c).

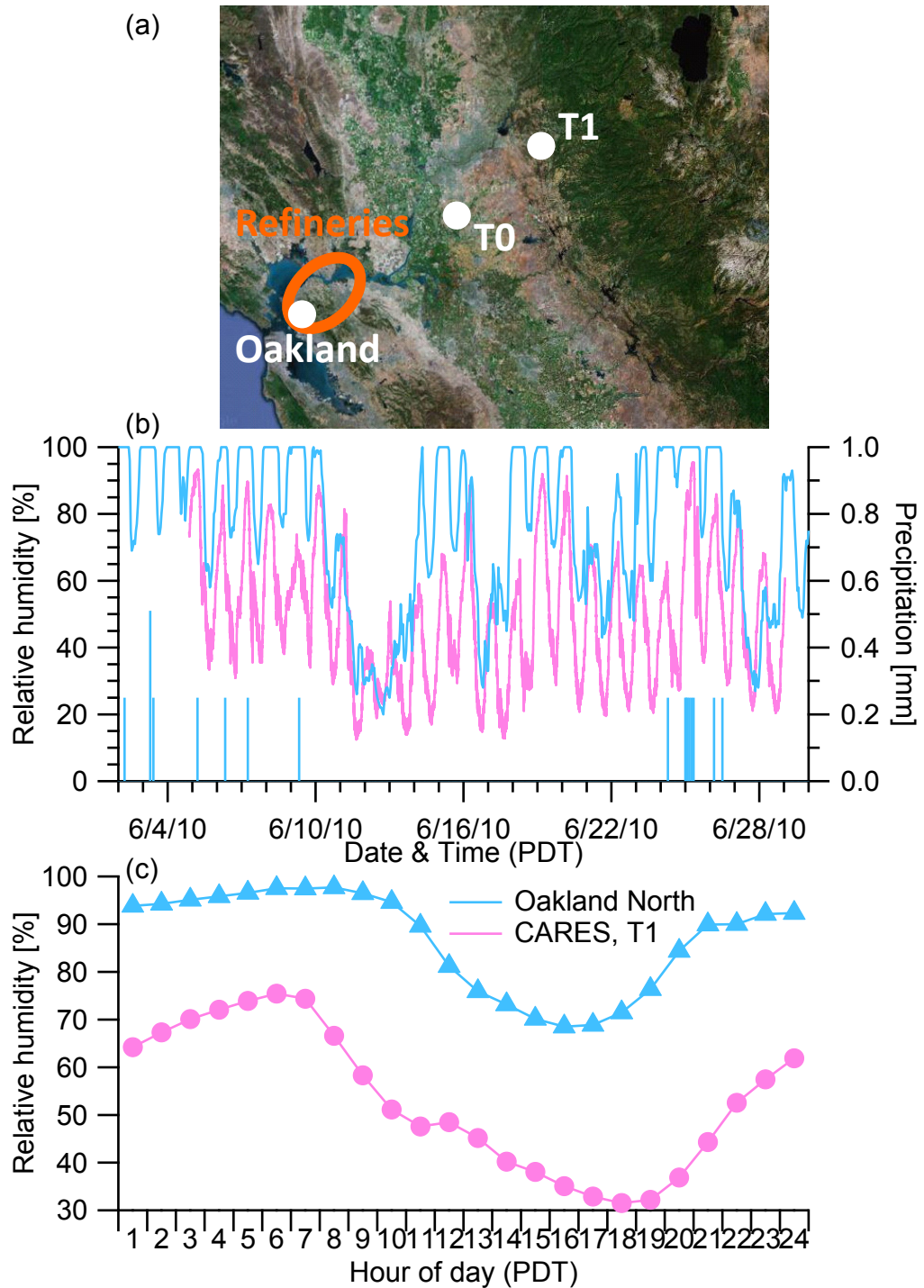


**Figure S5.** Summary of the evaluation of the PMF results: **(a)**  $Q/Q_{\text{exp}}$  as a function of number of factors (P); **(b)**  $Q/Q_{\text{exp}}$  as a function of fPeak values for the 3-factor solution; **(c)** fractions of OA factors as a function of fPeak values; **(d)** correlation between the 3 OA components in terms of mass spectrum and time series (1: biogenic SOA, 2: urban transport, 3: HOA); **(e)**  $Q/Q_{\text{exp}}$  values for each ion; **(f)** box plot of the scaled residuals for each ion; **(g)** time series of the measured organic mass concentration and the reconstructed organic mass (= biogenic SOA + urban transport + HOA); **(h)** time series of the residual (= measured - reconstructed) of the fit; **(i)** time series of  $Q/Q_{\text{exp}}$  (adapted from Zhang et al., 2011).

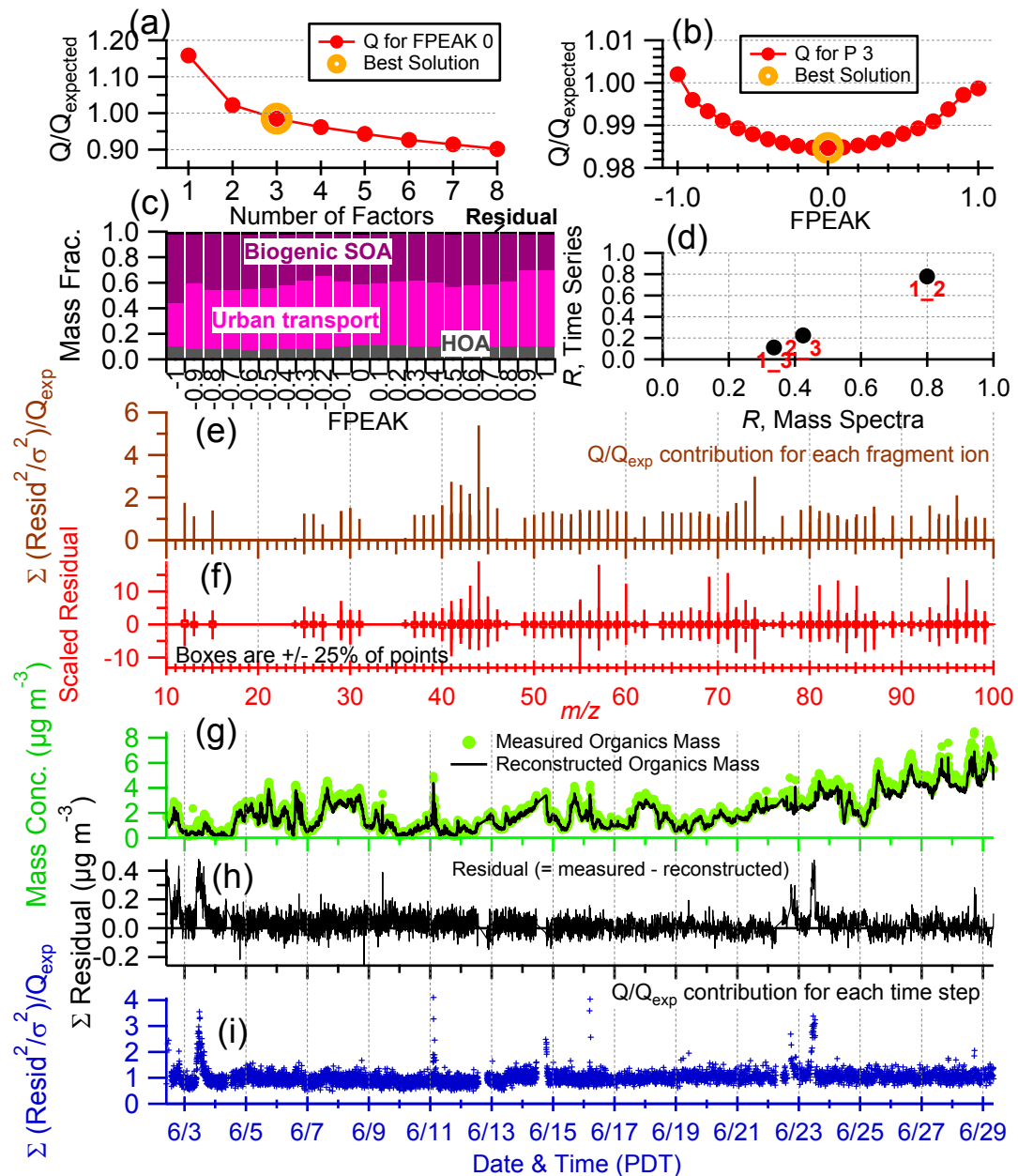


**Figure S6.** High resolution mass spectra and time series of OA components for the 2-factor solution (**a**, **b**) and 4-factor solution (**c**, **d**).

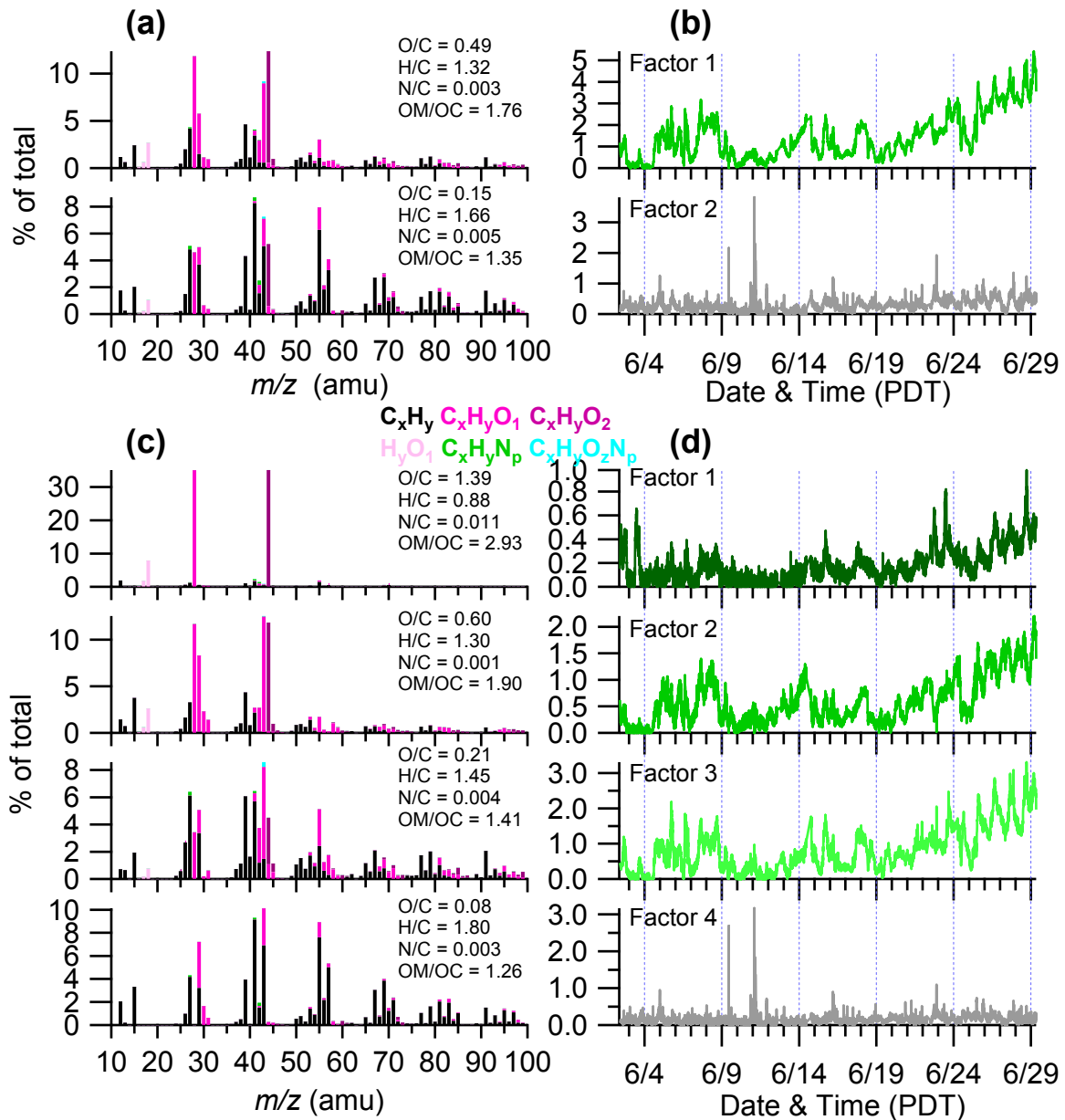


**Figure S7.** Mass spectra (in unit mass resolution) of BSOAs from CARES, Chebogue Pt (Canada) (correlation coefficient vs. CARES BSOA:  $r^2 = 0.95$ ) and plant chamber experiments ( $r^2 = 0.97$ ; Kiendler-Scharr et al., 2009) **(a)**, and those of CARES urban transport SOA and average OOA from multiple ambient data sets (correlation coefficient vs. CARES urban transport SOA:  $r^2 = 0.95$ ; Ng et al., 2011) **(b)**. Original reference mass spectra have been modified by scaling signals at  $m/z$  16, 17, 18 and 28 to that of  $m/z$  44 ( $m/z$  28 =  $m/z$  44;  $m/z$  18 =  $0.225 \cdot m/z$  44;  $m/z$  17 =  $0.25 \cdot 0.225 \cdot m/z$  44;  $m/z$  16 =  $0.04 \cdot 0.225 \cdot m/z$  44).

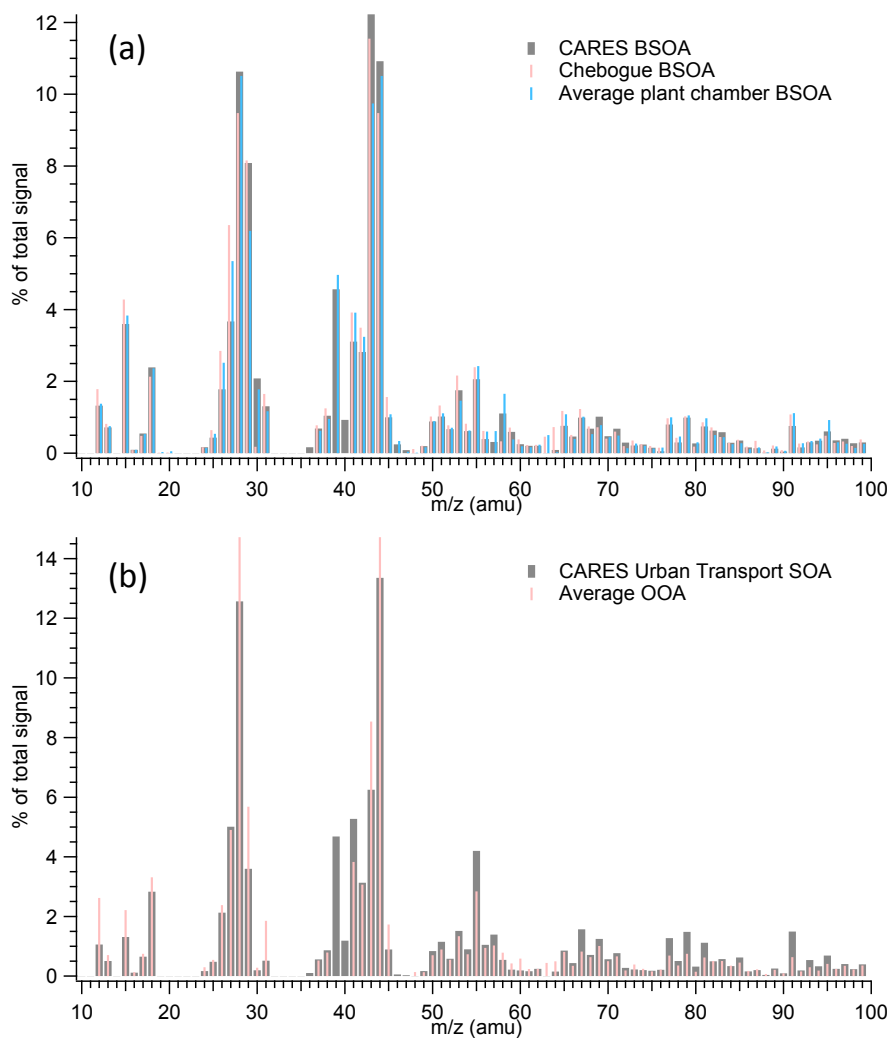


**Figure S8.** Scatterplots of (a) MACR+MVK vs. MO-OOA, (b) O<sub>3</sub> vs. LO-OOA, (c) black carbon vs. HOA, and (d) CO vs. HOA. All the scatterplots are colored by time and the data fittings were performed using the orthogonal distance regression (ODR).

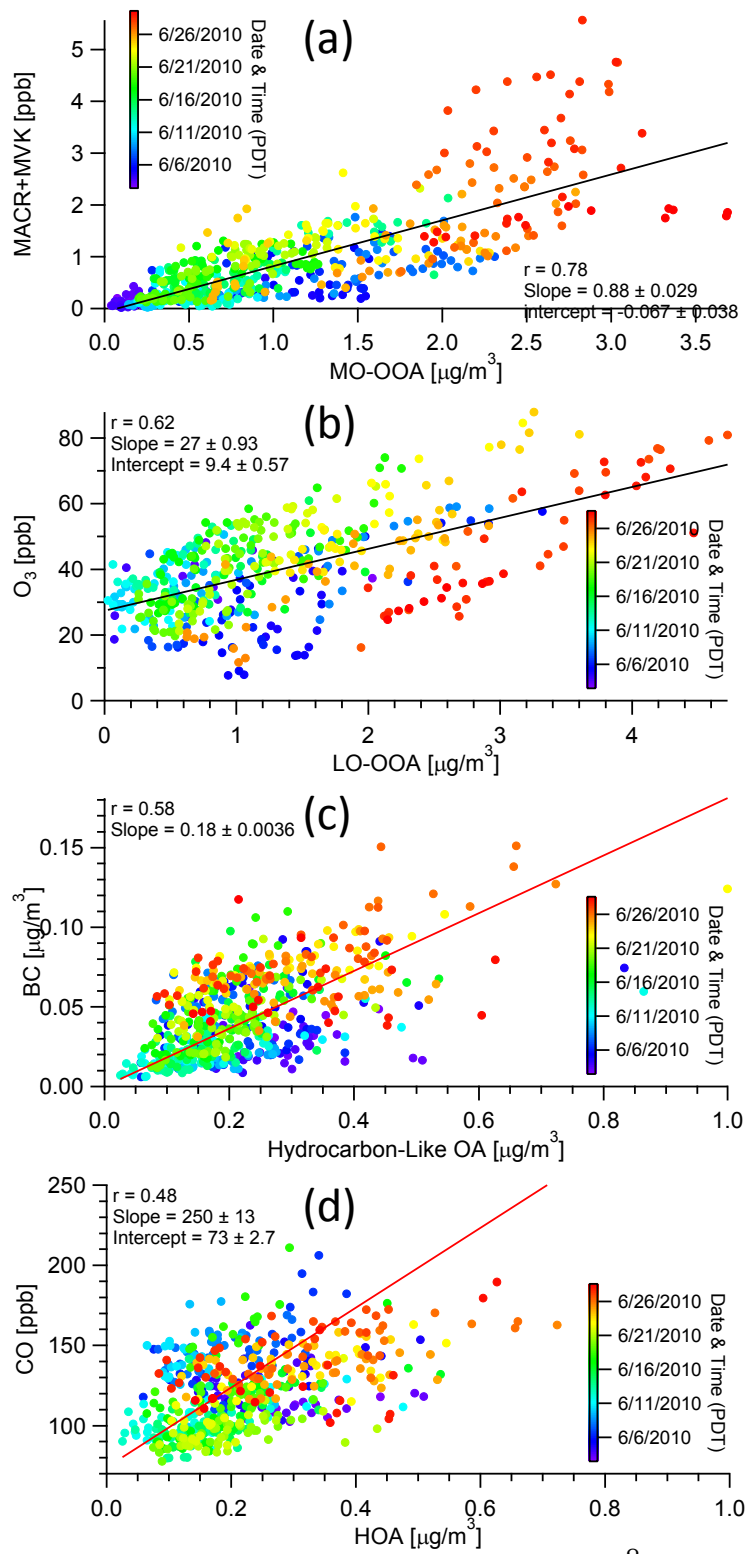


**Figure S9.** Correlation coefficients ( $r^2$ ) between OA factors and ions, colored by ion families (a, b, c). High resolution mass spectra of the OA factors, colored by ion families (d, e, f).

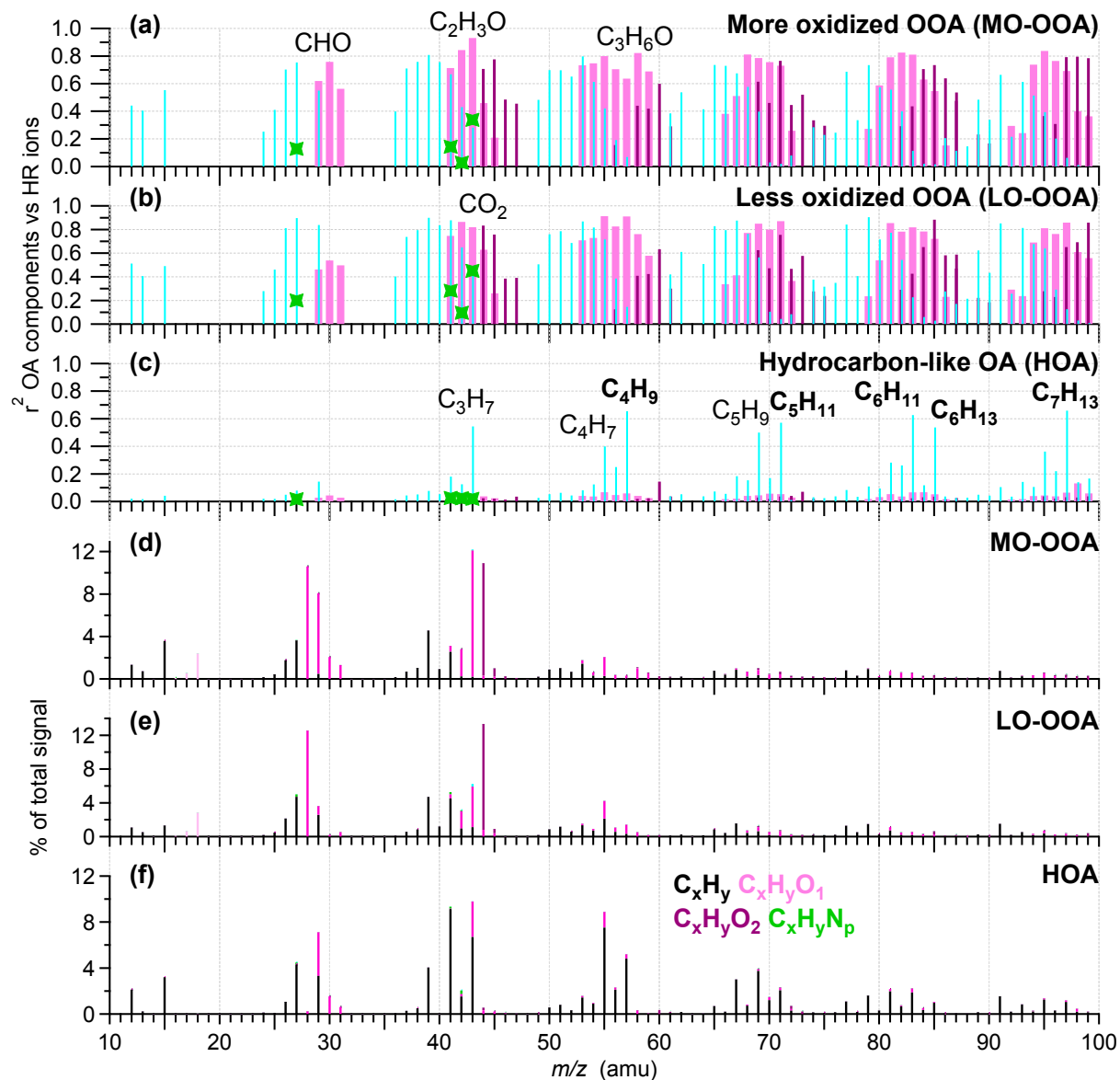


**Figure S10.** Triangle plot ( $f_{CO_2}$  vs.  $f_{C_2H_3O}$ ) with ambient data (colored by time) and OA components. The triangle region has been determined by Ng et al. (2010) and corresponds to region where ambient OOA components from different datasets fall. Red star points correspond to OOA components previously published and reporting biogenic influences (Allan et al., 2006; Williams et al., 2007; Cottrell et al., 2008; Sun et al., 2009; Raatikainen et al., 2010; Slowik et al., 2010).

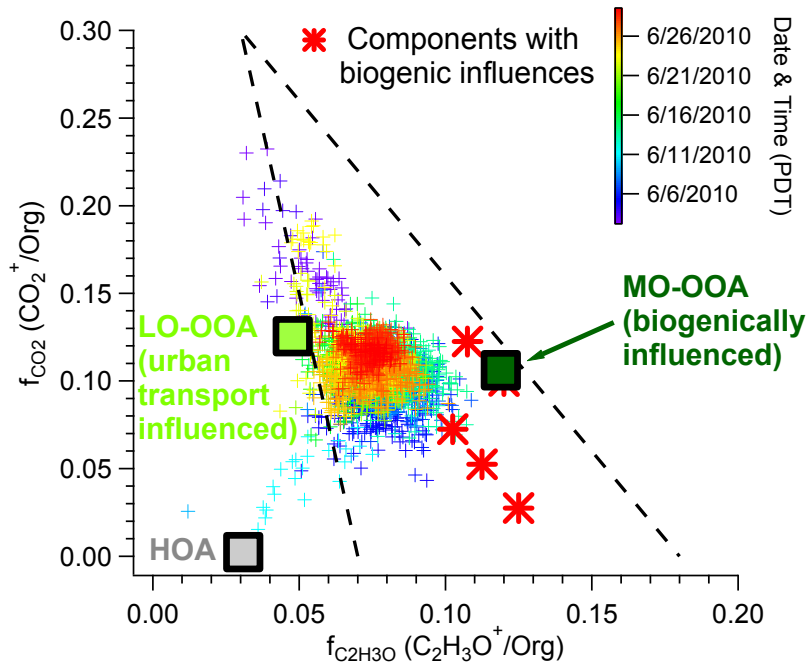


**Figure S11.** Scatterplot of methanol vs. acetone, colored by air mass types. The data fitting was performed using the orthogonal distance regression (ODR).

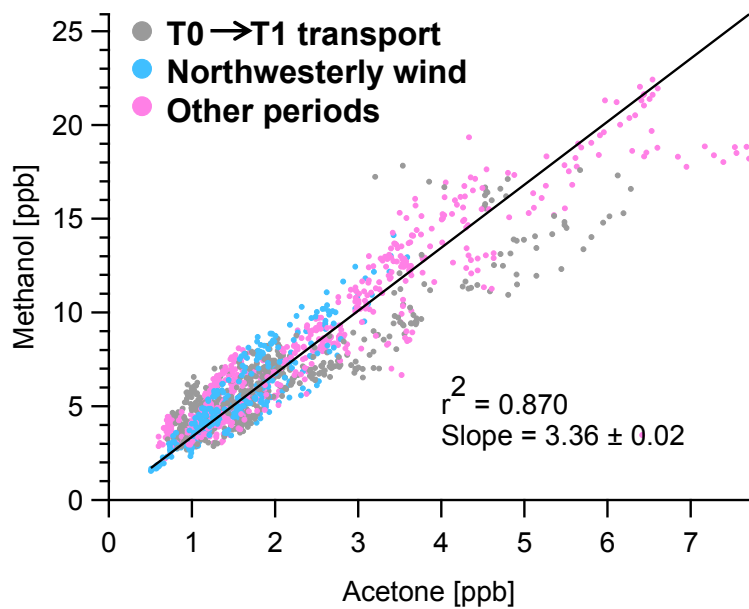
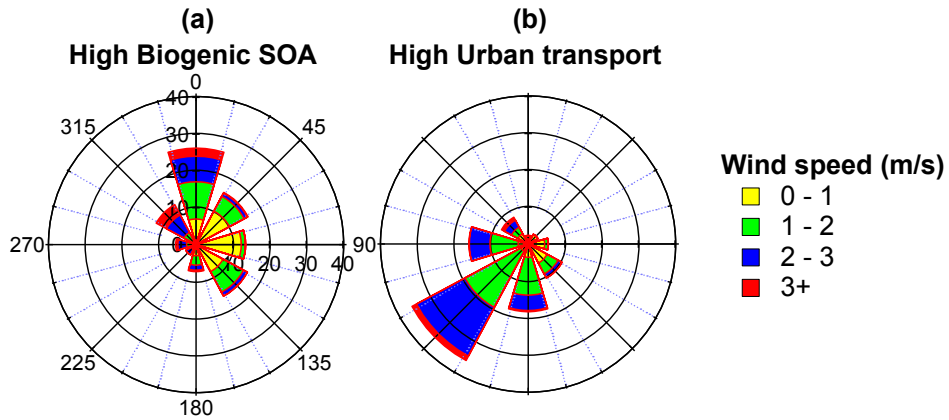


**Figure S12.** Wind rose plots (colored by wind speed, height: 3 m) for periods during which (a) biogenic SOA and (b) urban transport accounted for more than 60% of the total organic mass. The corresponding wind rose plot for HOA is not shown, because HOA dominated the total organic mass only during a few isolated data acquisitions. Radial scales correspond to the frequency, and are kept the same in the two wind roses.



## References

- Allan, J. D., Alfarra, M. R., Bower, K. N., Coe, H., Jayne, J. T., Worsnop, D. R., Aalto, P. P., Kulmala, M., Hytönen, T., Cavalli, F., and Laaksonen, A.: Size and composition measurements of background aerosol and new particle growth in a Finnish forest during QUEST 2 using an Aerodyne Aerosol Mass Spectrometer, *Atmos. Chem. Phys.*, 6, 315-327, 10.5194/acp-6-315-2006, 2006.
- Cottrell, L. D., Griffin, R. J., Jimenez, J. L., Zhang, Q., Ulbrich, I., Ziemba, L. D., Beckman, P. J., Sive, B. C., and Talbot, R. W.: Submicron particles at Thompson Farm during ICARTT measured using aerosol mass spectrometry, *J. Geophys. Res.-Atmos.*, 113, D08212, 10.1029/2007jd009192, 2008.
- Kiendler-Scharr, A., Zhang, Q., Hohaus, T., Kleist, E., Mensah, A., Mentel, T. F., Spindler, C., Uerlings, R., Tillmann, R., and Wildt, J.: Aerosol Mass Spectrometric Features of Biogenic SOA: Observations from a Plant Chamber and in Rural Atmospheric Environments, *Environ. Sci. Technol.*, 43, 8166-8172, 10.1021/es901420b, 2009.
- Ng, N. L., Canagaratna, M. R., Zhang, Q., Jimenez, J. L., Tian, J., Ulbrich, I. M., Kroll, J. H., Docherty, K. S., Chhabra, P. S., Bahreini, R., Murphy, S. M., Seinfeld, J. H., Hildebrandt, L., Donahue, N. M., DeCarlo, P. F., Lanz, V. A., Prevot, A. S. H., Dinar, E., Rudich, Y., and Worsnop, D. R.: Organic aerosol components observed in Northern Hemispheric datasets from Aerosol Mass Spectrometry, *Atmos. Chem. Phys.*, 10, 4625-4641, 10.5194/acp-10-4625-2010, 2010.
- Ng, N. L., Canagaratna, M. R., Jimenez, J. L., Zhang, Q., Ulbrich, I. M., and Worsnop, D. R.: Real-Time Methods for Estimating Organic Component Mass Concentrations from Aerosol Mass Spectrometer Data, *Environ. Sci. Technol.*, 45, 910-916, 10.1021/es102951k, 2011.
- Raatikainen, T., Vaattovaara, P., Tiitta, P., Miettinen, P., Rautiainen, J., Ehn, M., Kulmala, M., Laaksonen, A., and Worsnop, D. R.: Physicochemical properties and origin of organic groups detected

in boreal forest using an aerosol mass spectrometer, *Atmos. Chem. Phys.*, 10, 2063-2077, 10.5194/acp-10-2063-2010, 2010.

Slowik, J. G., Stroud, C., Bottenheim, J. W., Brickell, P. C., Chang, R. Y. W., Liggio, J., Makar, P. A., Martin, R. V., Moran, M. D., Shantz, N. C., Sjostedt, S. J., van Donkelaar, A., Vlasenko, A., Wiebe, H. A., Xia, A. G., Zhang, J., Leaitch, W. R., and Abbatt, J. P. D.: Characterization of a large biogenic secondary organic aerosol event from eastern Canadian forests, *Atmos. Chem. Phys.*, 10, 2825-2845, 10.5194/acp-10-2825-2010, 2010.

Sun, Y. L., Zhang, Q., Macdonald, A. M., Hayden, K., Li, S. M., Liggio, J., Liu, P. S. K., Anlauf, K. G., Leaitch, W. R., Steffen, A., Cubison, M., Worsnop, D. R., van Donkelaar, A., and Martin, R. V.: Size-resolved aerosol chemistry on Whistler Mountain, Canada with a high-resolution aerosol mass spectrometer during INTEX-B, *Atmos. Chem. Phys.*, 9, 3095-3111, 10.5194/acp-9-3095-2009, 2009.

Williams, B. J., Goldstein, A. H., Millet, D. B., Holzinger, R., Kreisberg, N. M., Hering, S. V., White, A. B., Worsnop, D. R., Allan, J. D., and Jimenez, J. L.: Chemical speciation of organic aerosol during the International Consortium for Atmospheric Research on Transport and Transformation 2004: Results from in situ measurements, *J. Geophys. Res.-Atmos.*, 112, D10S26, 10.1029/2006jd007601, 2007.

Zhang, Q., Jimenez, J., Canagaratna, M., Ulbrich, I., Ng, N., Worsnop, D., and Sun, Y. L.: Understanding atmospheric organic aerosols via factor analysis of aerosol mass spectrometry: a review, *Analytical and Bioanalytical Chemistry*, 401, 3045-3067, 10.1007/s00216-011-5355-y, 2011.